Supplementary Information

Engineering Vacancy-Defective Carbon Nitride Nanowire Clusters for Dramatically Enhanced Visible-Light-Driven Photocatalytic H_2O_2 Production

Ziyi Liao [a,b], Huilin Hou [a,], Jingjing Du [b], Lin Wang [a], Shuhua Wang [a], Shuo Wang [a], Xiaoqiang Zhan [a], Hongli Yang [a], Dongjiang Yang [a] and Weiyou Yang [a,*]*

[a] Institute of Micro/Nano Materials and Devices, Ningbo University of Technology, Ningbo City, 315211, P.R. China.

[b] College of Packaging and Materials Engineering, Hunan University of Technology, Zhuzhou City, 412007, P. R. China.

* Corresponding Emails: houhuilin86@163.com (H. Hou); weiyouyang@tsinghua.org.cn (W. Yang)

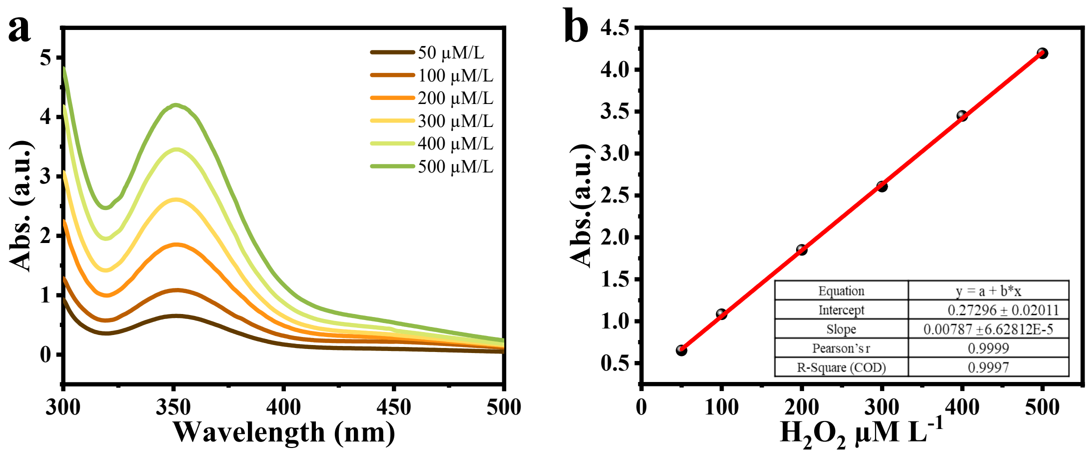

Fig. S1 (a) The absorbance of standard H_2O_2 solutions of different concentrations in the UV-vis spectrum determined by iodometric method, (b) Correspondence curve between absorbance and H_2O_2 concentration by linear fit, the inserted table shows the fitting results.

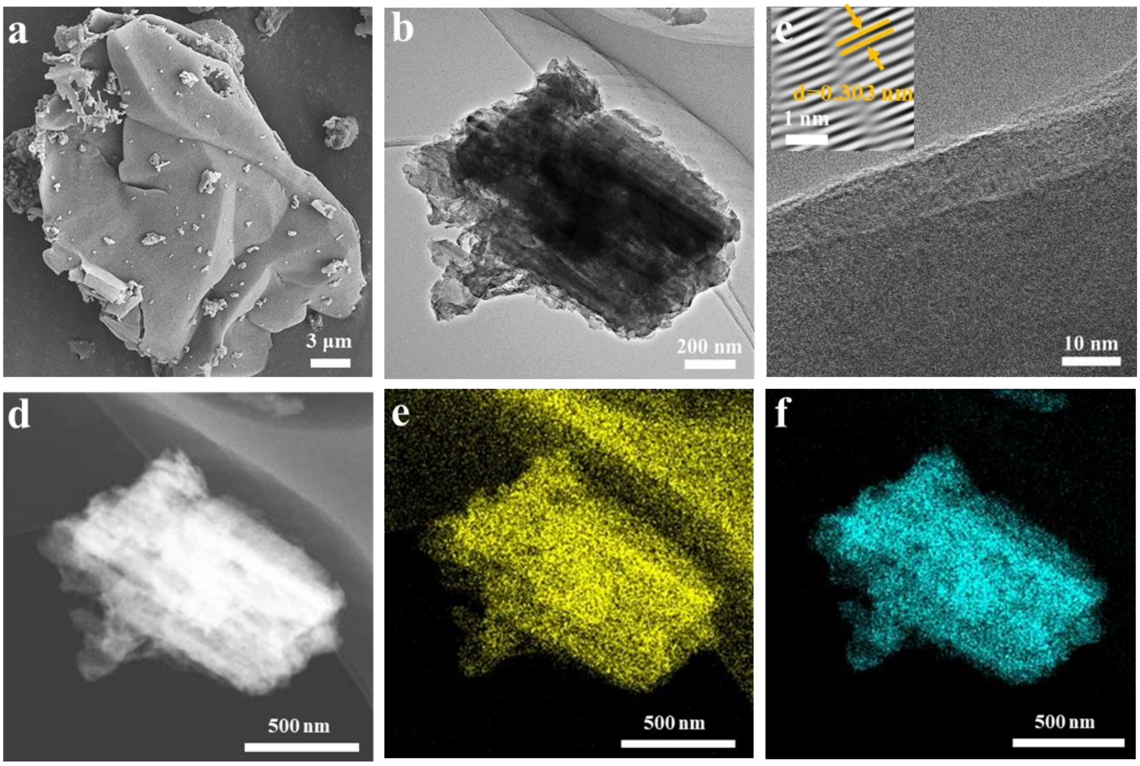

Fig. S2 Representative SEM image (a), TEM image (b), HRTEM image (c) and element mapping (d-f) of MACN.

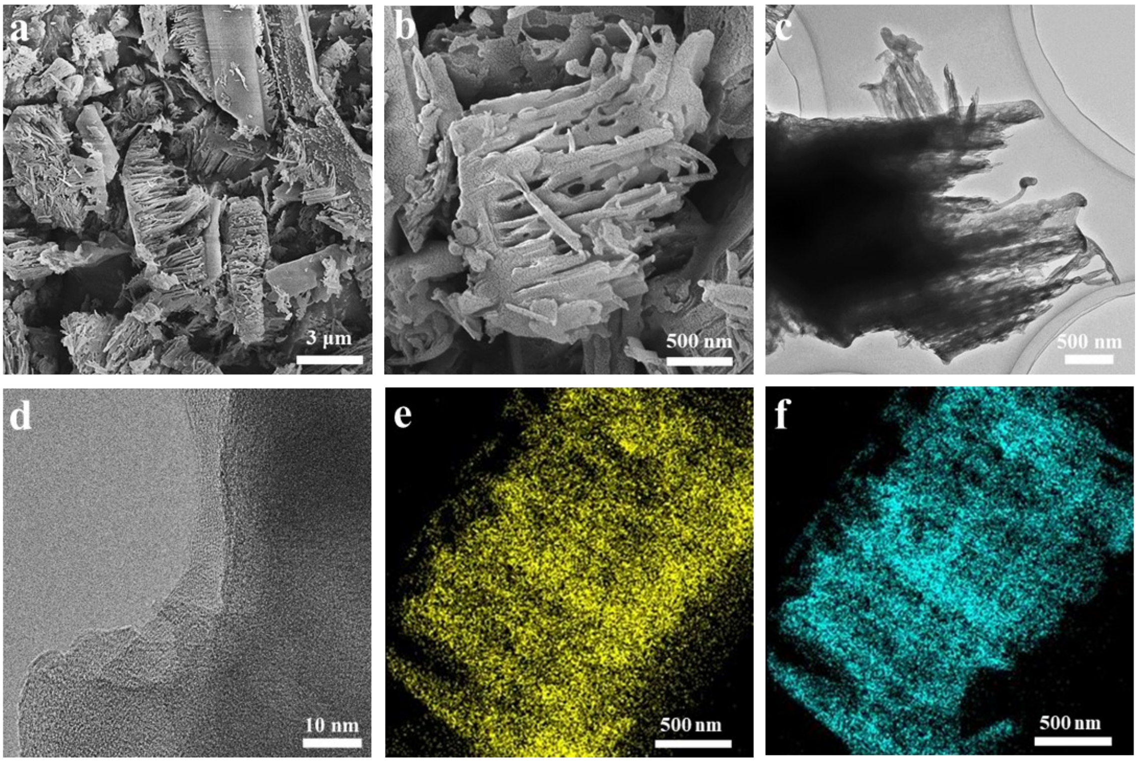

Fig. S3 Representative SEM images (a-b), TEM image (c), HRTEM image (d) and element mapping (e-f) of MCN.

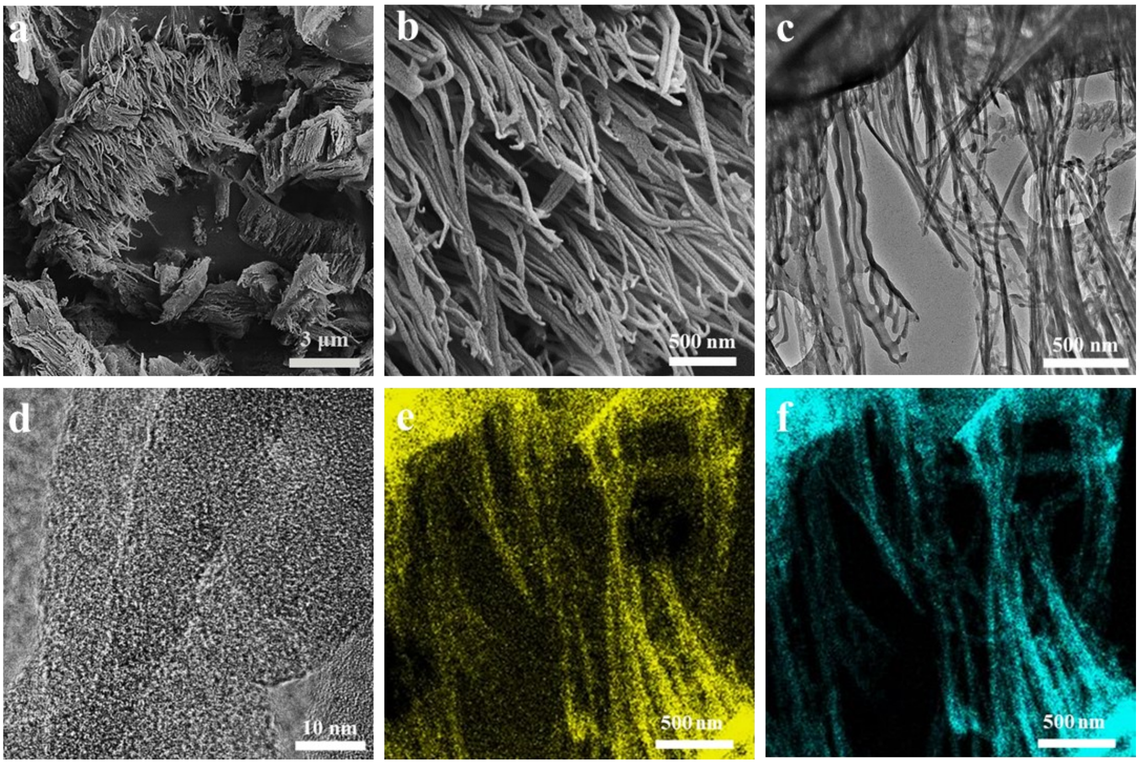

Fig. S4 Representative SEM images (a-b), TEM image (c), HRTEM image (d) and element mapping (e-f) of MNCN.

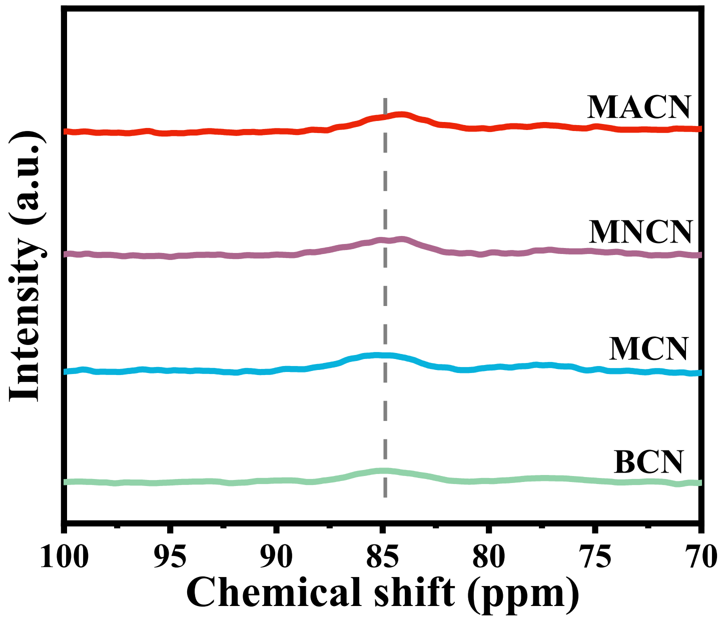

Fig. S5 Localized enlargement of Solid-state ^{13}C NMR spectra of BCN, MCN, MNCN and MACN, respectively.

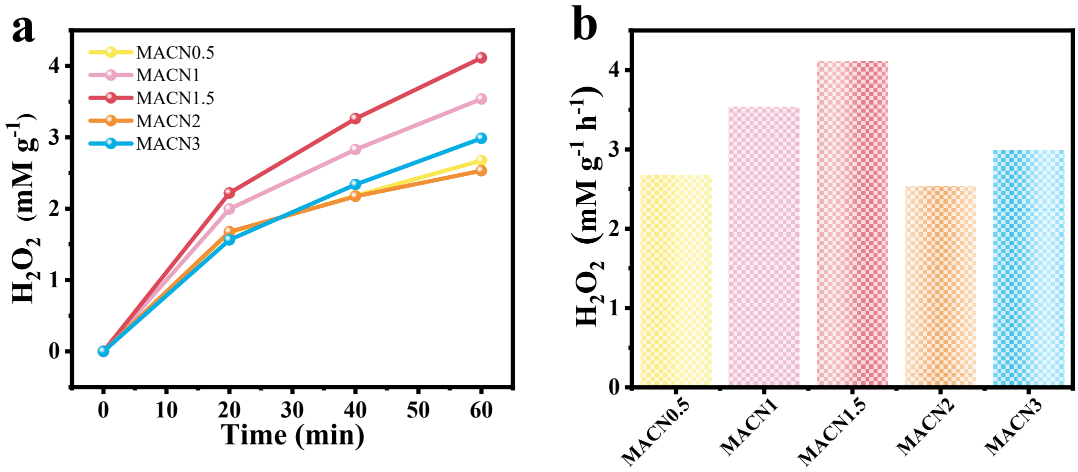

Fig. S6 (a) Photocatalytic H_2O_2 production of MACN at different heat treatment times ($\lambda \geq$ 420nm, 5 mg of photocatalyst, 10% IPA, 25℃), (b) Comparison of the photocatalytic H_2O_2 generation activity of different samples under the same conditions.

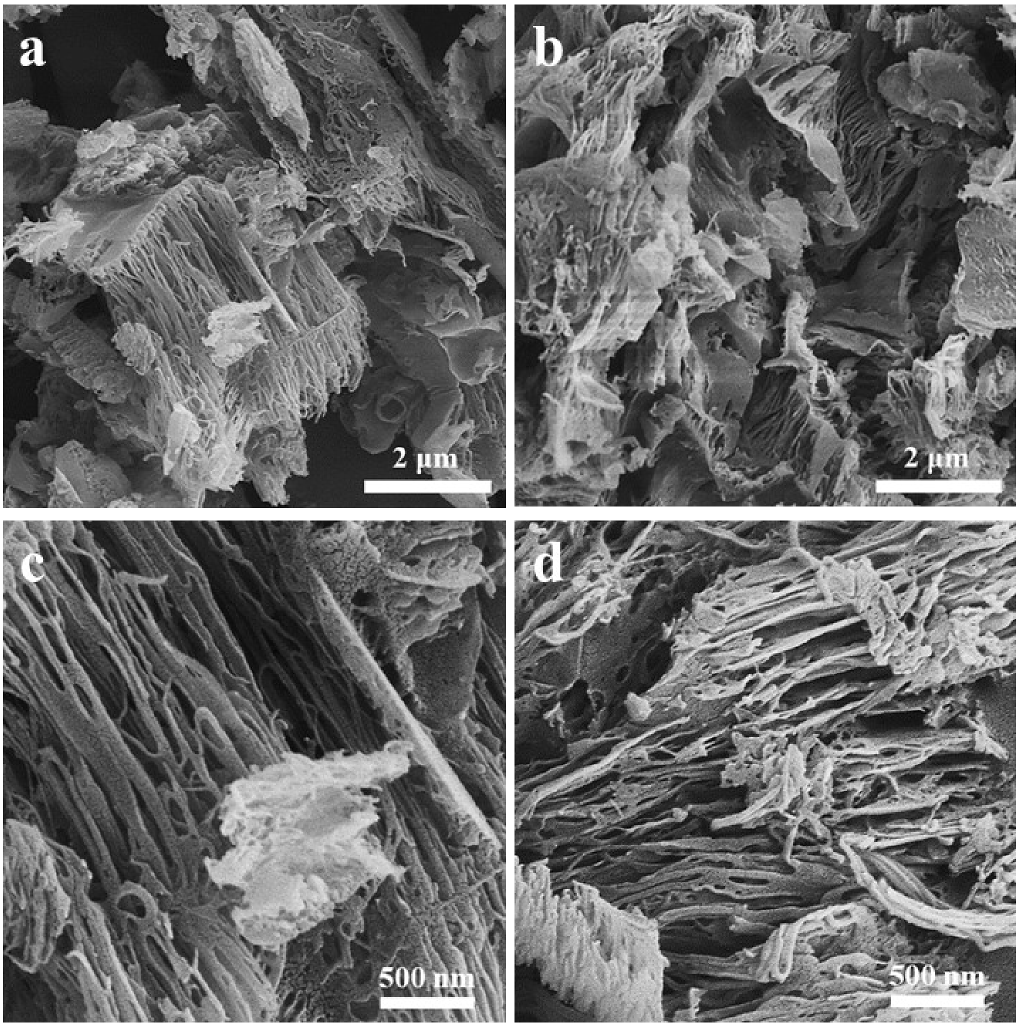

Fig. S7 SEM images of MACN after cycling tests.

.

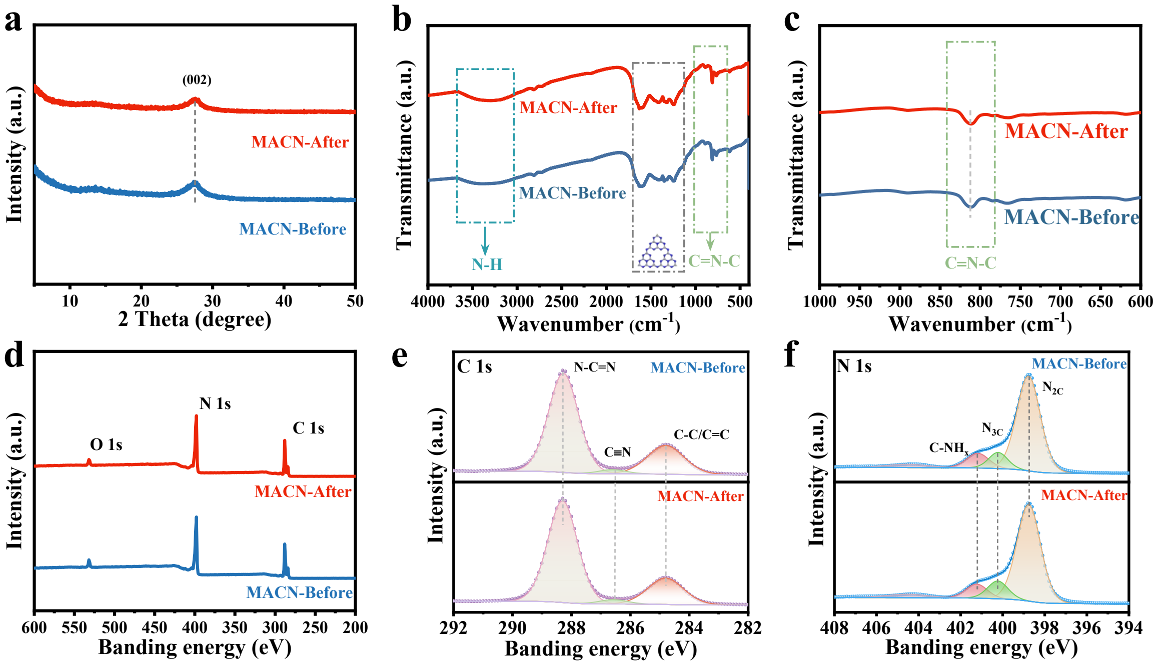

Fig. S8 Comparison of the MACN catalyst before and after the cycling tests: (a) XRD patterns, (b) FT-IR spectra, (c) Localized enlargement of FT-IR spectra, (d) XPS survey spectra, (e) High-resolution C 1s XPS spectra, and (f) High-resolution N 1s XPS spectra.

Table S1. Photocatalytic performance of H_2O_2 generation for recently fabricated g-C_3N_4 with defected.

Photocatalyst	**H_2O_2 generation rates (mmol h^{-1} g^{-1})**	**Light power and filter**	**Sacrificial agent**	**Reference**
UCNS580	4.17	420 nm 300 W Xe lamp	EtOH	[1]
MACN	4.11	420 nm 300 W Xe lamp	IPA	This work
B-CNT	2.54	420 nm 300 W Xe lamp	IPA	[2]
CNT	2.48	420 nm 300 W Xe lamp	IPA	[2]
O-CNC4	2	420 nm 300 W Xe lamp	IPA	[3]
ACN	1.87	420 nm 300 W Xe lamp	IPA	[4]
Nv-CNN-3	1.78	420 nm 300 W Xe lamp	EtOH	[5]
OCN	1.2	420 nm 300 W Xe lamp	IPA	[6]
CNK0.2	1.01	420 nm 300 W Xe lamp	MeOH	[7]
Cv-PCNNS	0.98	420 nm 300 W Xe lamp	IPA	[8]
H-CN	0.72	420 nm 300 W Xe lamp	IPA	[9]
g-C_3N_4-0.05	0.704	420 nm 300 W Xe lamp	IPA	[10]
Cv-g-C_3N_4	0.5	420 nm 300 W Xe lamp	None	[11]
SPCN	0.32	420 nm 300 W Xe lamp	IPA	[12]
Cv-CN	0.28	420 nm 300 W Xe lamp	IPA	[13]
CN-ND	0.2	420 nm 300 W Xe lamp	MeOH	[14]
Nv-C≡N-CN	0.14	420 nm 300 W Xe lamp	None	[15]
PCN-NVc	0.03	420 nm 300 W Xe lamp	MeOH	[16]

Table S2. Fitting results of time-resolved photoluminescence spectroscopy (TRPL) acquired from BCN, MCN, MNCN and MACN.

Sample	τ_1	**Rel %**	τ_2	**Rel %**	τ_3	**Rel %**	τ_{avg}
BCN	0.91	19.69	3.32	51.16	14.13	29.15	2.56
MCN	0.93	16.14	3.26	45.70	12.73	38.16	2.91
MNCN	0.83	4.63	3.90	31.50	15.38	63.87	5.62
MACN	1.01	5.56	4.28	32.07	17.29	62.37	6.03

References

1 J. Shi, H. Wang, J. Nie, T. Yang, C. Ju, K. Pu, J. Shi, T. Zhao, H. Li, J. Xue, *J. Colloid Interface Sci.,* 2023, **643***,* 47-61.

2 Y. Liu, Y. Zheng, W. Zhang, Z. Peng, H. Xie, Y. Wang, X. Guo, M. Zhang, R. Li, Y. Huang, *Sci. Technol.,* 2021, **95**, 127-135.

3 H. Xie, Y. Zheng, X. Guo, Y. Liu, Z. Zhang, J. Zhao, W. Zhang, Y. Wang, Y. Huang, *ACS Sustainable Chem. Eng.,* 2021, **9**, 6788-6798.

4 Y. Zheng, Y. Luo, Q. Ruan, S. Wang, J. Yu, X. Guo, W. Zhang, H. Xie, Z. Zhang, Y. Huang, *Appl. Catal., B.,* 2022, **311**, 121372.

5 C. Zhao, C. Shi, Q. Li, X. Wang, G. Zeng, S. Ye, B. Jiang, J. Liu, *Mater. Today Energy*, 2022, **24**, 100926.

6 Z. Wei, M. Liu, Z. Zhang, W. Yao, H. Tan, Y. Zhu, *Energy Environ. Sci.,* 2018, **11**, 2581-2589.

7 Y. Wang, D. Meng, X. Zhao, *Appl. Catal., B.*, 2020, **273**, 119064.

8 R. Li, M. Zheng, X. Zhou, D. Zhang, Y. Shi, C. Li, M. Yang, *Chem. Eng. J.,* 2023, **464**, 142584.

9 Z. Zhang, Y. Zheng, H. Xie, J. Zhao, X. Guo, W. Zhang, Q. Fu, S. Wang, Q. Xu, Y. Huang, *J. Alloys Compd.,* 2022, **904**, 164028.

10 H. Zhang, L. Jia, P. Wu, R. Xu, J. He, W. Jiang, *Appl. Surf. Sci.,* 2020, **527**, 146584.

11 X. Xu, Y. Xu, Y. Liang, H. Long, D. Chen, H. Hu, J. Ou, *Mater. Chem. Front.,* 2022, **6**, 3143-3173.

12 W. Miao, Y. Wang, Y. Liu, H. Qin, C. Chu, S. Mao, *Engineering,* 2023, **25**, 214-221.

13 J. Han, M. Song, Y. Li, Y. Yao, S. Lu, X. Liao, *React. Chem. Eng.,* 2024, **9**, 148-159.

14 H. Fattahimoghaddam, T. Mahvelati-Shamsabadi, B. Lee, *ACS Sustainable Chem. Eng.,* 2021, **9**, 4520-4530.

15 X. Zhang, P. Ma, C. Wang, L. Gan, X. Chen, P. Zhang, Y. Wang, H. Li, L. Wang,

X. Zhou, K. Zheng, *Energy Environ. Sci.,* 2022, **15**, 830-842.

16 F. Lin, T. Wang, Z. Ren, X. Cai, Y. Wang, J. Chen, J. Wang, S. Zang, F. Mao, L. Lv, *J. Colloid Interface Sci.,* 2023, **636**, 223-229.